

## BIOGENIC ZnO NANOPARTICLES: STRUCTURAL CHARACTERISATION AND BIOACTIVITY EVALUATION

Abhimanyu Parasram Pawar <sup>ORCID</sup><sup>a\*</sup>, Kishor Sudhir Naktode <sup>ORCID</sup><sup>a</sup>, Arvind Janardhan Mungole <sup>ORCID</sup><sup>b</sup>,  
Srinivas Anga <sup>ORCID</sup><sup>c</sup>

<sup>a</sup>Department of Chemistry, Nevjabai Hitkarini College, Khed Road, Bramhapuri, dist. Chandrapur, Maharashtra 441 206, India

<sup>b</sup>Department of Botany, Nevjabai Hitkarini College, Khed Road, Bramhapuri, dist. Chandrapur, Maharashtra 441 206, India

<sup>c</sup>Department of Chemistry, Koneru Lakshmaiah Education Foundation, Bachupally-Gandimaisamma Road, Bowrampet, Hyderabad, Telangana-500043, India

\*e-mail: pawarabhay909@gmail.com

**Abstract.** Zinc oxide nanoparticles were synthesized via a green route using *Nicotiana plumbaginifolia* plant extract, serving as a novel bio-reducing and stabilizing agent. Structural analysis through X-ray diffraction confirmed the hexagonal wurtzite crystalline structure, while Fourier-transform infrared spectroscopy and energy-dispersive X-ray spectroscopy affirmed the presence of Zn–O bonds and high purity. Morphological characterization by scanning electron microscopy and transmission electron microscopy revealed spherical nanoparticles with sizes ranging from 16 to 24 nm. The calculated optical band gap was 3.33 eV. A prominent FTIR peak at 480 cm<sup>-1</sup> indicated Zn–O stretching vibrations. The Zinc oxide nanoparticles exhibited significant antibacterial activity against *Pseudomonas aeruginosa* (18 mm), *Escherichia coli* (19 mm), *Klebsiella pneumoniae* (19 mm), and *Staphylococcus aureus* (18 mm) at 100 µL, as evaluated by the well diffusion method. Additionally, the nanoparticles showed strong antioxidant activity, achieving 75.59% DPPH radical scavenging at 250 µg/mL, indicating potential biomedical applications.

**Keywords:** Green synthesis, ZnO nanoparticle, EDX, FT-IR, SEM, antibacterial activity, antioxidant activity.

Received: 23 April 2025/ Revised final: 16 June 2025/ Accepted: 19 June 2025

### Introduction

Nanoscience has revolutionised various industries, including pharmaceuticals, cosmetics, textiles, and electronics, due to the unique properties of nanomaterials [1,2]. Defined by their nanoscale dimensions (1–100 nm), these materials exhibit exceptional physicochemical, optical, and mechanical properties, making them valuable for applications in energy storage, catalysis, biosensors, and biomedical fields [3-5]. The high surface area-to-volume ratio and quantum confinement effects of nanoparticles enable functionalities that surpass those of bulk materials [6,7]. Among metal and metal oxide nanoparticles, zinc oxide (ZnO) has gained significant attention due to its antimicrobial, antioxidant, and anticancer properties, along with its applications in optoelectronics and catalysis [8-10]. However, conventional ZnO NP synthesis involves energy-intensive methods and toxic by-products, raising environmental concerns [11,12]. Green synthesis using plant extracts offers a sustainable alternative, where phytochemicals such as flavonoids, alkaloids, and phenolics act as natural reducing and stabilising agents [13-15].

While several plant species have been explored, including *Aquilegia pubiflora* [16], *Lupinus albus* [17], *Evolvulus alsinoides* [18], *Zingiber officinale* [19], and *Vinca rosea* [20]. These plants are chosen for their high content of bioactive compounds, which facilitate nanoparticle synthesis. Compared to these species, *Nicotiana plumbaginifolia* offers a unique advantage due to its rich phytochemical profile, particularly in alkaloids and phenolics, which can enhance the reduction and stabilisation of ZnO NPs. Despite this potential, the application of *N. plumbaginifolia* in ZnO NP synthesis remains underexplored, positioning this study as a novel contribution to green nanotechnology.

This study aims to explore the green synthesis of ZnO nanoparticles using *N. plumbaginifolia* extract and to evaluate their antibacterial and antioxidant activities. The novelty lies in employing this plant for the first time as a bioreducing agent for ZnO NP synthesis, providing an eco-friendly and cost-effective route. The synthesised nanoparticles are characterised and assessed for their potential applications in biomedicine, biosensing, and environmental remediation.

## Experimental

### Materials

The selected botanical specimen, *Nicotiana plumbaginifolia*, was sourced from the proximate Bramhapuri region in the Chandrapur district of Maharashtra state, India. The plant material was meticulously collected and utilised in extract preparation. Sigma-Aldrich supplied zinc nitrate hexahydrate ( $\text{Zn}(\text{NO}_3)_2 \cdot 6\text{H}_2\text{O}$ ) as a zinc precursor and 1,1-diphenyl-2-picrylhydrazyl (DPPH), butylated hydroxytoluene (BHT) ensuring high-grade chemical standards for the experiments. Amikacin 30  $\mu\text{g}$  and butylated hydroxytoluene served as positive controls in antibacterial and antioxidant assays, respectively.

### Preparation of extracts from whole plant material

The *Nicotiana plumbaginifolia* (Viv.) plant material used in this study was sourced from an area near Bramhapuri town in the Chandrapur district, Maharashtra, India. Upon collection, the plant material was thoroughly washed with deionised water multiple times (two to three rinses) to remove any dirt or contaminants. After the cleaning process, the plant was sliced into smaller pieces and dried in a shaded area to prevent degradation from direct sunlight. Once fully dried, the plant was ground into a fine powder using a mortar and pestle.

To prepare the extract, 20 g of the powdered plant material was placed into a clean, dry round-bottom flask, and 200 mL of distilled water was added. The mixture was then heated and boiled for at least 30 minutes to extract the bioactive compounds. After boiling, the solution was allowed to cool to ambient temperature. The cooled solution was filtered through Whatman number 41 filter paper to obtain a clear filtrate. This filtrate was then stored in an airtight conical flask and refrigerated for future use in the nanoparticle synthesis process.

### Biosynthesis of zinc oxide nanoparticles

The synthesis of zinc oxide nanoparticles was conducted in accordance with a procedure adapted from the method described [21]. In this approach, 100 mL of *Nicotiana plumbaginifolia* (Viv.) plant extract was introduced into a round-bottom flask (RBF) and subjected to thermal treatment using a magnetic stirrer, with the temperature maintained between 70–80°C. To this, a 30 mL aqueous solution of zinc nitrate hexahydrate (3 g) was incrementally added to the reaction mixture under continuous agitation. The solution was then allowed to undergo reflux until a highly viscous, deep yellow colloidal substance, exhibiting adhesive characteristics, was formed. This product was meticulously

separated and transferred into a ceramic crucible for further processing. The collected material was subsequently subjected to calcination in a muffle furnace at 500°C for a duration of 2 hours. Post-calcination, the resultant product was a fine, whitish or light-coloured powder of ZnO nanoparticles. These nanoparticles were then processed and utilised for subsequent structural and functional characterisation.

### Characterization techniques of nanoparticles

Zinc oxide nanoparticles were thoroughly characterised using a range of analytical techniques. The morphological features and size of the nanoparticles were examined using scanning electron microscopy (SEM) coupled with energy dispersive X-ray spectroscopy (EDS) for elemental composition analysis. Transmission electron microscopy (TEM) was employed to further analyse the particle size and morphology. The crystallographic properties of the ZnO NPs were evaluated using X-ray diffraction (XRD) with a Bruker AXS D8 system. To investigate the optical properties and functional groups, Fourier transform infrared (FTIR) spectroscopy was performed using a Thermo Nicolet iS50 FTIR spectrometer, while UV-Visible spectroscopy was carried out with a Thermo Scientific Evolution 300 UV-Visible spectrophotometer to confirm the formation of nanoparticles. Additionally, X-ray absorption spectroscopy was utilised to determine the elemental composition and electronic structure of the ZnO NPs.

All characterisation analyses were conducted at the Sophisticated Analytical Instrument Facility (SAIF), Kochi, India, ensuring accurate and comprehensive evaluation of the synthesised ZnO nanoparticles.

### Antioxidant and antibacterial screening of ZnO nanoparticles

The antioxidant activity of the synthesized ZnO nanoparticles (NPs) was evaluated by assessing their ability to scavenge the 1,1-diphenyl-2-picrylhydrazyl (DPPH) free radical. ZnO NPs, synthesized using *Nicotiana plumbaginifolia*, were tested at varying concentrations (20, 40, 60, 80, and 100  $\mu\text{g}/\text{mL}$ ). Each concentration was prepared by mixing 3 mL of methanol with 1 mL of a 4% DPPH solution in equal volumes at ambient temperature. The resulting mixtures were incubated in the dark for 30 minutes to allow for the reaction to occur.

Following incubation, the absorbance of each solution was measured at 517 nm using a visible spectrophotometer. Positive control butylated hydroxytoluene (BHT) was used as a reference standard for comparison. Samples of

each concentration were tested in triplicate and the average absorption was taken.

The percentage of radical scavenging activity (% RSA) was calculated according to the following Eq.(1).

$$\% RSA = \left[ \frac{(A_{control} - A_{sample})}{A_{control}} \right] \times 100 \quad (1)$$

where, %RSA - the percentage of radical scavenging activity, and also denotes absorbance;

$A_{control}$  - the absorbance of the sample at time zero, measured at 517 nm;

$A_{sample}$  - the absorbance of the sample, measured at 517 nm.

Antibacterial screening represents a fundamental approach for evaluating the inhibitory effects of compounds against microbial pathogens. A variety of laboratory techniques are available for assessing antibacterial activity, with the agar dilution and disc diffusion methods being the most prevalently utilised. In the present study, the antibacterial potential of the synthesized ZnO nanoparticles (NPs) was systematically assessed at concentrations of 25, 50, and 100  $\mu$ L against a panel of four clinically relevant bacterial strains: *Escherichia coli* (*E. coli*), *Staphylococcus aureus* (*S. aureus*), *Pseudomonas aeruginosa* (*P. aeruginosa*), and *Klebsiella pneumoniae* (*K. pneumoniae*). The antibacterial efficacy was quantitatively determined by measuring the zone of inhibition surrounding the impregnated discs containing the ZnO NPs. These results were compared to the activity of the reference antibiotic, Amikacin (30  $\mu$ g), serving as a positive control. The extent of the inhibition zone was employed as an indicator of the bacteriostatic and bactericidal capabilities of the ZnO NPs against the aforementioned bacterial strains.

The omission of negative controls in our antimicrobial assays was based on precedent in the existing literature on plant-mediated ZnO nanoparticles. Numerous studies report that common solvents used in such biosynthetic processes do not exhibit intrinsic antimicrobial or antioxidant activity, thus having minimal influence on the final biological assessment [22,23]. Consequently, solvent-only or extract-only negative controls are often not included in our study.

## Results and discussion

### DR spectra analysis

The optical diffuse reflectance (DR) spectra of the synthesized zinc oxide nanoparticles (ZnO NPs) were recorded in the wavelength range of 200–1100 nm, with measurements conducted in reflection mode, as depicted in Figure 1(a). The reflectance spectra revealed a notable sharp increase at approximately 376 nm, followed by a pronounced reflective peak around 450 nm, which is characteristic of ZnO NPs. This observation aligns with previously reported findings [24]. The fundamental electronic transitions, including the excitation of electrons from the valence band to the conduction band, are instrumental in determining the optical bandgap. The excitation of electrons across the bandgap is a critical factor in enhancing the photocatalytic activity of the synthesised nanoparticles. To calculate the optical bandgap energy, a plot of  $(F(R)hv)^2$  versus  $hv$  (where  $hv$  represents photon energy in eV) was constructed for the biosynthesised ZnO NPs derived from *Nicotiana plumbaginifolia*, as shown in Figure 1(b). The calculated bandgap energy for the ZnO NPs was determined to be 3.33 eV, which is consistent with the typical range for ZnO nanomaterials and indicates their potential for photocatalytic applications.

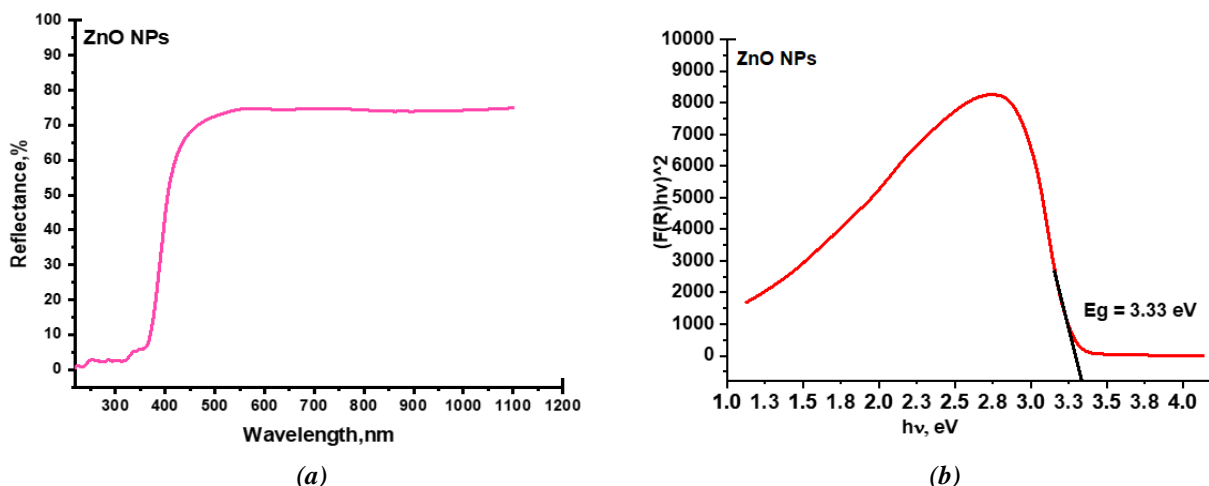


Figure 1. Diffuse reflectance spectrum (a), Plot of  $(F(R)hv)^2$  versus  $hv$  (eV) (b) for ZnO NPs prepared.

### Fourier transform infrared spectroscopy analysis

The Fourier transform infrared (FTIR) spectroscopic analysis was conducted to identify the functional groups of the biomolecules implicated in the capping and stabilisation of the synthesised zinc oxide nanoparticles (ZnO NPs). The FTIR spectra of the synthesised ZnO NPs, as depicted in Figure 2(a) reveal several distinctive absorption bands corresponding to various functional groups. A prominent absorption at  $480\text{ cm}^{-1}$  is indicative of the Zn–O stretching vibration, which is characteristic of the ZnO framework, confirming the successful synthesis of ZnO NPs [25]. Further analysis of the spectra reveals an absorption band at  $3423\text{ cm}^{-1}$ , which can be attributed to the O–H stretching vibration of hydroxyl groups, commonly found in polyphenolic compounds [26]. The band at  $1629\text{ cm}^{-1}$  corresponds to the C=O stretching vibration associated with carboxyl (COOH) functional groups [27]. The peak at  $1384\text{ cm}^{-1}$  is attributed to the bending vibration of the C–N group, while the peaks observed at  $1149\text{ cm}^{-1}$  and  $1029\text{ cm}^{-1}$  are indicative of C–OH stretching and C–H bending vibrations, respectively. The absorption at  $674\text{ cm}^{-1}$  corresponds to the C–H stretching vibration of alkene groups [28]. These spectral features suggest the presence of polyphenolic compounds, carboxyl groups, amine (CN) groups, and alcohol functionalities (C–OH), which are likely involved in the reduction, stabilization, and capping of the ZnO NPs. These biomolecules may play a crucial role in modulating the size, stability, and surface characteristics of the synthesised nanoparticles, thus enhancing their potential for various applications.

### X-ray diffraction and energy dispersive X-ray spectroscopy

The crystalline structure of the green-synthesised ZnO NPs derived from *Nicotiana plumbaginifolia* (Viv.) was analysed using X-ray diffraction (XRD), as shown in Figure 2(b). The diffraction peaks observed at  $2\theta$  values of  $31.785^\circ$ ,  $34.498^\circ$ ,  $36.289^\circ$ ,  $47.577^\circ$ ,  $56.617^\circ$ ,  $62.942^\circ$ ,  $66.351^\circ$ ,  $68.032^\circ$ ,  $69.098^\circ$ , and  $73.628^\circ$  were indexed to the corresponding diffraction planes (100), (002), (101), (102), (110), (103), (200), (112), (201), and (004), respectively. These experimental results of peaks align extremely well with the XRD pattern of hexagonal wurtzite structure for the ZnO nanoparticles having JCPDS or IDCC no. 00-036-1451 [29] from the documented as

illustrated in Figure 2(b). The crystallographic parameters of zinc oxide were determined using Rietveld analysis of the XRD data with the help of specialized software. The unit cell parameters were found to be  $a = b = 3.2498\text{ \AA}$  and  $c = 5.2066\text{ \AA}$ , with  $\alpha = \beta = 90^\circ$  and  $\gamma = 120^\circ$ , confirming a hexagonal structure with the  $P6_3mc$  space group.

To estimate the average crystallite or particle size ( $D$ ) of the synthesised ZnO nanoparticles, the Debye-Scherrer equation was employed, which is given by:  $D = k \cdot \lambda / (\beta \cos \theta)$ , where  $D$  represents the average crystallite size,  $k$  is the shape factor with a value of 0.94,  $\lambda$  is the X-ray wavelength ( $\lambda = 1.54\text{ \AA}$ ),  $\beta$  is the full width half maximum (FWHM) value in radians, and  $\theta$  is the Bragg's angle.

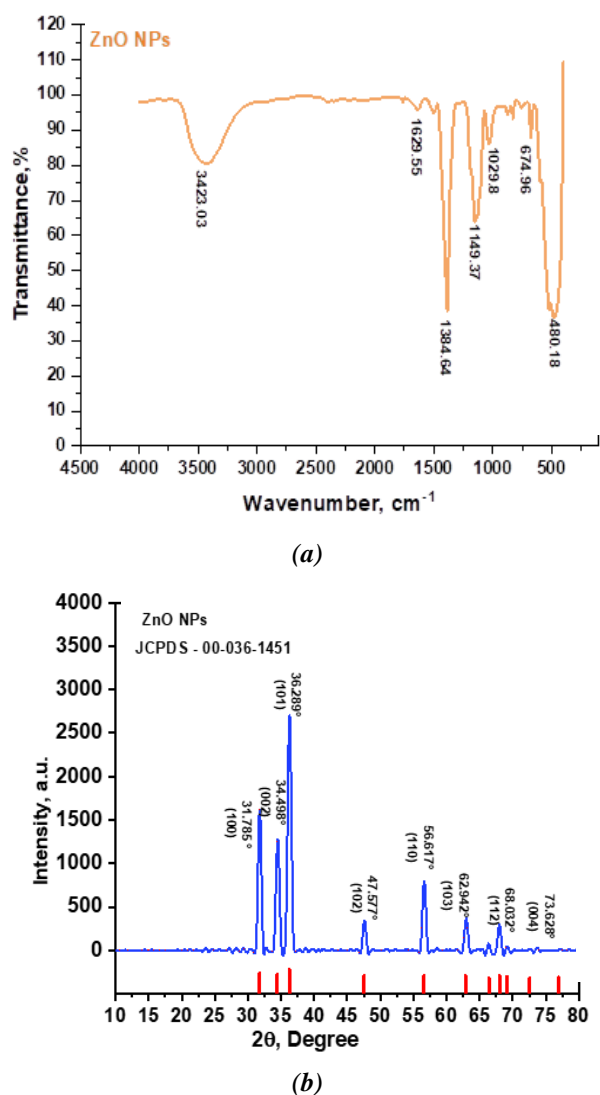


Figure 2. FTIR (a) and XRD spectrum (b) of synthesised Zinc Oxide nanoparticles.

The average crystallite size of the synthesized ZnO NPs was calculated to be 14.95 nm. The nanoparticles exhibited a crystallinity of 82.08%, reflecting a substantial level of crystalline purity. Moreover, the dislocation density was found to be 0.005392, which quantifies the number of crystal lattice defects present within the sample. The interplanar spacing ( $d$ ) values, corresponding to the various diffraction planes, were also determined, as outlined in Table 1. These findings provide critical insights into the structural characteristics of the ZnO NPs, corroborating their crystalline structure and aiding in the understanding of their material properties.

#### Scanning electron microscopy (SEM)

The morphological characteristics of the synthesized ZnO nanoparticles were analysed using Scanning electron microscopy (SEM), as presented in Figure 3(a) and (b). The SEM micrographs revealed that the ZnO nanoparticles predominantly exhibited a spherical morphology. However, notable agglomeration was observed, with particles forming compact clusters and displaying non-uniform spatial distribution [30].

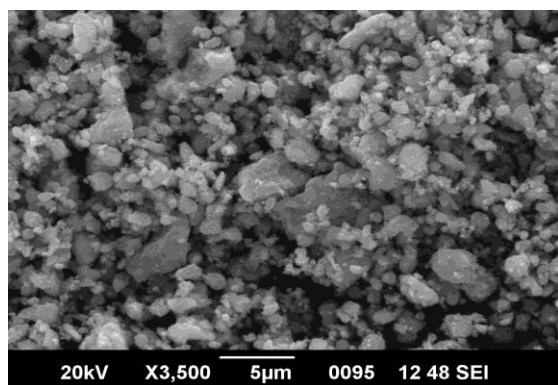
Such agglomeration is commonly associated with biogenic synthesis methods. A primary contributing factor is the presence of residual phytochemicals from the *Nicotiana plumbaginifolia* extract, which, while serving as reducing and stabilizing agents, can also promote interparticle interactions leading to aggregation. In addition, van der Waals forces and hydrogen bonding among surface-bound biomolecules further enhance agglomeration, particularly during drying or post-synthesis handling.

#### Transmission electron microscopy (TEM)

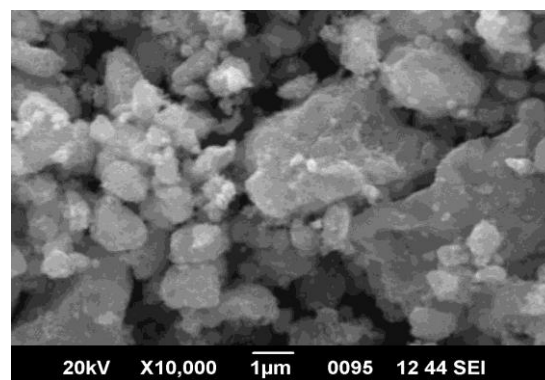
Transmission electron microscopy (TEM) was utilised to ascertain the precise structural configuration and size distribution of the ZnO nanoparticles synthesised *via* the biogenic route using *Nicotiana plumbaginifolia* (Viv.) plant extract. The TEM micrographs, presented in Figure 4(a) and (b), confirm the formation of ZnO nanoparticles with a predominantly spherical morphology [31] and an average particle size ranging from 16 to 24 nm. Additionally, the Selected Area Electron Diffraction (SAED) pattern further substantiates the crystalline nature of the synthesised ZnO nanoparticles.

Table 1

Crystallite size (D) and interplanar spacing (d) of formed ZnO NPs were calculated.							
Plane	$2\theta$ (Degree)	FWHM	Crystallite size (D) nm	$\theta$ value (Degree)	Interplanar Spacing(d) (Å)	Dislocation Density $\delta=1/D^2$	Crystallinity
(100)	31.786	0.626	12.755	15.893	2.813	0.006	82.082
(002)	34.498	0.694	11.421	17.249	2.598	0.008	
(101)	36.278	0.633	12.466	18.139	2.474	0.006	
(102)	47.578	0.693	10.956	23.789	1.910	0.008	
(110)	56.617	0.679	18.754	28.309	1.624	0.003	
(103)	62.943	0.905	17.819	31.471	1.475	0.003	
(200)	66.351	0.766	19.069	33.176	1.408	0.003	
(112)	68.031	0.843	18.161	34.016	1.377	0.003	
(201)	69.099	0.812	18.414	34.549	1.358	0.003	
(004)	73.629	0.684	9.705	36.814	1.285	0.011	



(a)



(b)

Figure 3. Scanning electron microscopy images at 5 μm (a) and 1 μm (b).

The diffraction rings observed in the SAED pattern (Figure 5(a)), exhibit precise alignment with the diffraction peaks identified in the X-ray Diffraction (XRD) analysis thereby confirming the hexagonal wurtzite crystal structure of the ZnO nanoparticles. This congruence underscores the structural integrity and crystalline quality of the nanoparticles produced *via* this phytogenic synthesis approach.

#### The energy dispersive X-Ray diffraction analysis

The Energy Dispersive X-ray (EDX) spectroscopic analysis was conducted to determine the elemental composition of the synthesised ZnO nanoparticles, as illustrated in Figure 5(b). The EDX spectrum prominently displayed two strong peaks corresponding to zinc (Zn) and oxygen (O), confirming the successful formation of ZnO nanoparticles. Zinc was present at a weight

percentage of 51.65% and an atomic percentage of 28.13%, while oxygen was detected at 21.12% by weight and 47% by atomic percentage, verifying the stoichiometric presence of Zn and O in the nanostructure. Additionally, the spectrum showed minor peaks corresponding to chlorine (Cl) at 9.17% (weight) and 9.21% (atomic), potassium (K) at 11.87% (weight) and 10.81% (atomic), calcium (Ca) at 2.19% (weight) and 1.95% (atomic), copper (Cu) at 2.8% (weight) and 1.57% (atomic), and sulphur (S) at 1.2% (weight) and 1.33% (atomic). These trace elements likely originate from residual phytochemicals in the *Nicotiana plumbaginifolia* extract used during synthesis. Their presence suggests the involvement of bio-organic compounds in the reduction, stabilization, and possible functionalization of the ZnO nanoparticles, which is characteristic of green synthesis methods.

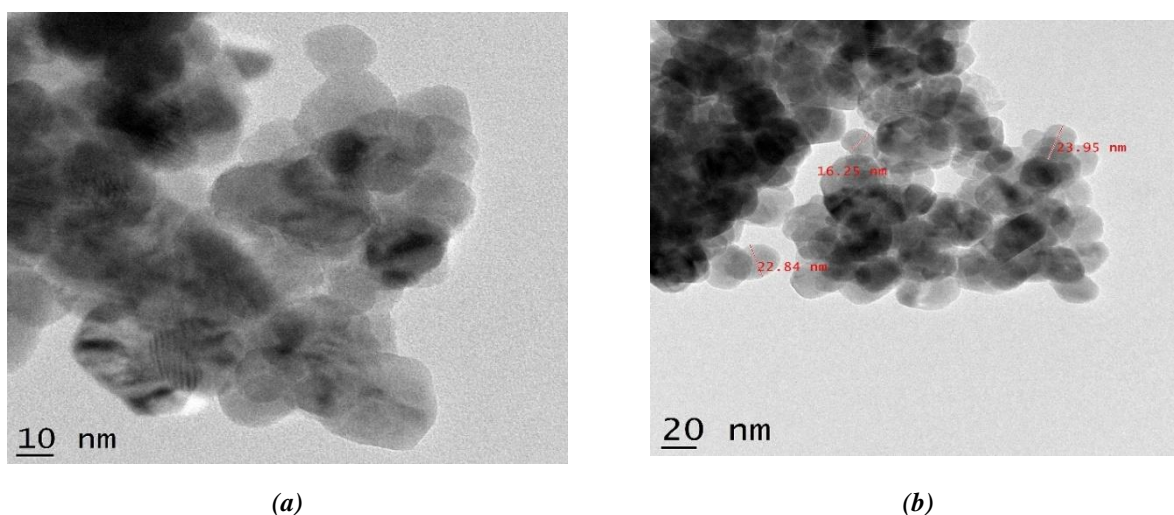


Figure 4. TEM Images of synthesized Zinc Oxide nanoparticles at 10 nm (a) and 20 nm scale (b).

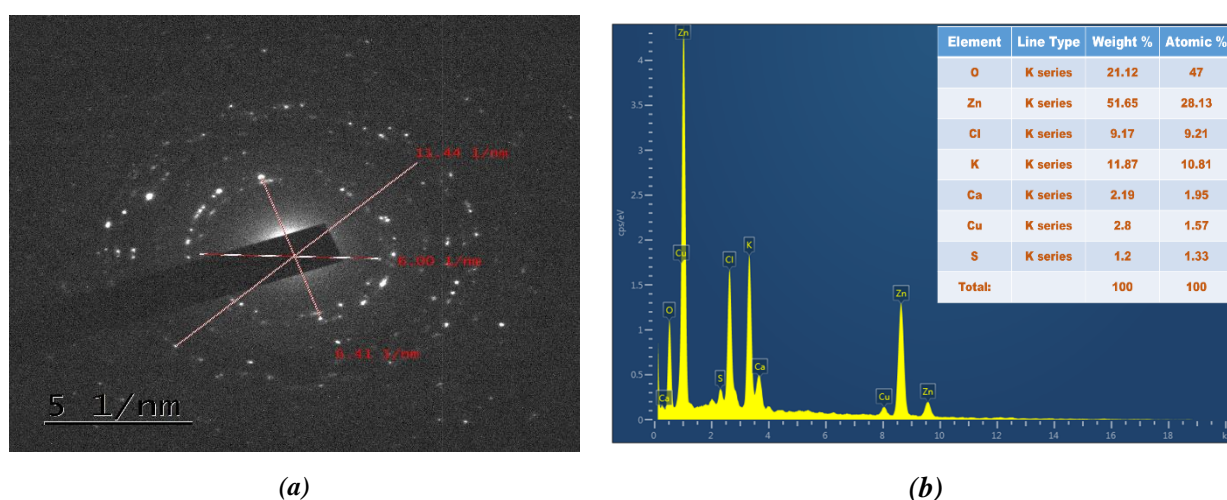


Figure 5. SAED pattern (a) and EDAX (b) images of synthesized nanoparticles.

### Antibacterial activity

The antibacterial efficacy of the synthesised ZnO nanoparticles (ZnO NPs) was rigorously assessed using the well-diffusion method, with detailed zones of inhibition (ZOI) recorded in Table 2. The study revealed differential susceptibilities among the tested bacterial strains. For *Escherichia coli*, amikacin exhibited a pronounced inhibitory effect, producing a 20 mm zone of inhibition. In comparison, ZnO NPs demonstrated concentration-dependent antibacterial activity, with inhibition zones measuring 13 mm, 17 mm, and 19 mm at 25  $\mu$ L, 50  $\mu$ L, and 100  $\mu$ L, respectively. Against *Staphylococcus aureus*, amikacin displayed strong antibacterial efficacy, yielding a 19 mm zone of inhibition. ZnO NPs also showed promising activity, with zones of inhibition measuring 14 mm, 16 mm, and 18 mm for the same concentrations. For *Pseudomonas aeruginosa*, amikacin achieved a 23 mm zone of inhibition, while ZnO NPs exhibited effective antibacterial activity with inhibition zones of 16 mm, 16 mm, and 18 mm at 25  $\mu$ L, 50  $\mu$ L, and 100  $\mu$ L, respectively. In the case of *Klebsiella pneumoniae*, amikacin produced a 20 mm zone of inhibition. ZnO NPs displayed comparable efficacy with inhibition zones of 16 mm, 18 mm, and 19 mm for the respective concentrations.

The antibacterial activity of ZnO NPs can be attributed to several mechanisms. One plausible

mechanism is the generation of reactive oxygen species (ROS) upon contact with bacterial cells, leading to oxidative stress, lipid peroxidation, and subsequent cell membrane damage, ultimately causing cell death [32].

These findings align with earlier studies [33-37] which explored the synthesis of zinc nanoparticles *via* plant extracts and highlighted their potent antibacterial activity against a range of bacterial strains. This investigation underscores the potential of ZnO NPs as an effective antimicrobial agent, demonstrating a concentration-dependent response and varying efficacy across different bacterial species when compared to amikacin. Table 3 provides a comprehensive summary of the antibacterial and antioxidant efficacy of ZnO nanoparticles synthesised in this investigation with various plant-derived methodologies documented in the existing literature. The biosynthesised ZnO nanoparticles demonstrated significant antimicrobial activity against *S. aureus*, achieving a maximum zone of inhibition (ZOI) measuring 18 mm at a concentration of 100  $\mu$ L, a result that is comparable to the findings of Al Bustany, A. *et al.*, [38] wherein green-synthesized ZnO nanoparticles attained a ZOI of 20 mm at a dosage of 100  $\mu$ L. Likewise, with respect to *E. coli*, our nanoparticles exhibited a ZOI of 19 mm, which is in close proximity to the 25 mm ZOI reported by Karatepe, P. *et al.* [39] employing a hydrothermal synthesis approach.

Table 2

**Zone of inhibition (ZOI) of organisms at various concentrations for ZnO NPs.**

Bacteria	ZOI (mm)			
	AK30*	25 $\mu$ L	50 $\mu$ L	100 $\mu$ L
<i>E. coli</i>	20	13	17	19
<i>S. aureus</i>	19	14	16	18
<i>P. aeruginosa</i>	23	16	16	18
<i>K. pneumoniae</i>	20	16	18	19

\*Standard antibiotic Amikacin 30  $\mu$ g.

Table 3

**Comparison of antibacterial activity (Zone of Inhibition, mm) of ZnO NPs.**

Bacteria	Size of nanoparticles	Concentration ( $\mu$ g/mL)	Zone of Inhibition (mm)	References
<i>K. pneumoniae</i>	23-25 nm	25 $\mu$ g	9 mm	[37]
<i>K. pneumoniae</i>	27.83 nm	50 $\mu$ g	18 mm	[35]
<i>K. pneumoniae</i>	52.50 nm	50 $\mu$ g	8 mm	[36]
<i>S. aureus</i>	23-25 nm	125 $\mu$ g	9 mm	[37]
<i>S. aureus</i>	14.25 nm	100 $\mu$ g	20 mm	[38]
<i>E. coli</i>	23-25 nm	50 $\mu$ g	25 mm	[39]
<i>E. coli</i>	14.25 nm	100 $\mu$ g	11.2 mm	[38]
<i>P. aeruginosa</i>	14.25 nm	200 $\mu$ g	13 mm	[38]
<i>p. aeruginosa</i>	52.50 nm	50 $\mu$ g	12.67 mm	[36]

### Antioxidant activity

Zinc oxide nanoparticles (ZnO NPs) synthesized from *Nicotiana plumbaginifolia* (Viv.) demonstrated significant antioxidant activity against 1,1-diphenyl-2-picrylhydrazyl (DPPH) radicals, as depicted in Figure 6. This observation is consistent with previous studies that have highlighted the antioxidant potential of ZnO NPs synthesised from various phytogetic sources [40,41]. In the present study, a concentration-dependent relationship was observed, with an incremental trend in antioxidant activity corresponding to increasing concentrations of ZnO NPs synthesised from *Nicotiana plumbaginifolia* (Viv.). The efficacy of ZnO nanoparticles, derived from diverse plant extracts, was evaluated through DPPH radical scavenging activity, serving as a measure of their antioxidant capabilities. In the present investigation, ZnO nanoparticles synthesized from *Nicotiana plumbaginifolia* (Viv.) exhibited a pronounced concentration-dependent scavenging effect, achieving an impressive maximum of 75.59% at a concentration of 250  $\mu\text{g/mL}$ . This value is significantly elevated in comparison to the antioxidant activity documented for *Scoparia dulcis* (54.02% at 250  $\mu\text{g/mL}$ ) and *Aloe fleurentinorum* (52.74% at 800  $\mu\text{g/mL}$ ), as indicated by the findings of Sivasankarapillai, V.S., et al. [42] and Jamil, Y.M. et al. [43].

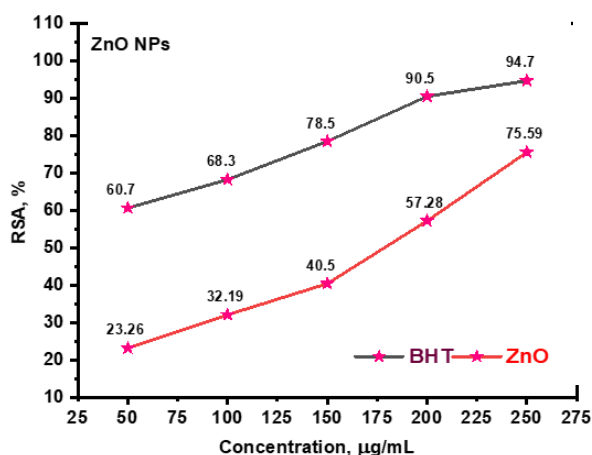


**Figure 6. Antioxidant activity of ZnO NPs green synthesised.**

These findings emphasize the remarkable antioxidant potential of ZnO NPs synthesized via the biogenic route using *Nicotiana plumbaginifolia* (Viv.) and their pronounced efficacy in a concentration-dependent manner. Moreover, ZnO NPs exhibit antioxidant properties by scavenging free radicals and reducing oxidative damage, which may indirectly contribute to their antibacterial efficacy [44]. Furthermore, the

superior performance of these nanoparticles relative to those synthesized from other botanical sources highlights their potential utility in nanoparticle-based antioxidant applications, offering valuable contributions to the domain of nanotechnology and functional material science.

### Conclusion

This study successfully demonstrates the green synthesis of zinc oxide nanoparticles (ZnO NPs) using *Nicotiana plumbaginifolia* extract as a bioreducing and stabilising agent. The phytochemicals present in the extract facilitated the reduction of zinc ions and stabilisation of the nanoparticles, offering a sustainable and cost-effective alternative to conventional synthesis methods. Structural and morphological characterisation through advanced spectroscopic and microscopic techniques confirmed the formation of predominantly spherical ZnO NPs. The novelty of this study lies in the utilization of *Nicotiana plumbaginifolia* as an eco-friendly source for nanoparticle synthesis, which not only addresses environmental concerns but also enhances the biocompatibility of ZnO NPs. Unlike traditional chemical synthesis methods, this green approach minimizes the use of toxic reagents and energy consumption, positioning it as a viable strategy for large-scale production. Furthermore, biological evaluation revealed significant antibacterial activity against pathogenic bacterial strains and strong antioxidant potential. These findings underscore the applicability of green-synthesised ZnO NPs in biomedical and industrial domains while reinforcing the viability of eco-friendly approaches in nanomaterial development.

### Acknowledgment

The authors express profound gratitude to the Principal of Nevjabai Hitkarini College, Bramhapuri, Maharashtra, India, for their unwavering support, encouragement, and the provision of essential facilities that significantly contributed to the successful execution of this research. Authors also extend heartfelt appreciation to the Sophisticated Test and Instrumentation Centre (STIC) at Cochin University of Science and Technology, Cochin, Kerala, India, for their invaluable assistance in the characterisation of the samples.

### References

- Malik, S.; Muhammad, K.; Waheed, Y. Nanotechnology: A revolution in modern industry. *Molecules*, 2023, 28(2), pp. 661–687. DOI: <https://doi.org/10.3390/molecules28020661>

2. Nasrollahzadeh, M.; Sajadi, S.M.; Sajjadi, M.; Issaabadi, Z. Applications of nanotechnology in daily life. *Interface Science and Technology*, 2019, 28, pp. 113–143. DOI: <https://doi.org/10.1016/B978-0-12-813586-0.00004-3>
3. Krifa, M.; Prichard, C. Nanotechnology in textile and apparel research - an overview of technologies and processes. *The Journal of The Textile Institute*, 2020, 111(12), pp. 1778–1793. DOI: <https://doi.org/10.1080/00405000.2020.1721696>
4. Payal; Pandey, P. Role of nanotechnology in electronics: A review of recent developments and patents. *Recent Patents on Nanotechnology*, 2022, 16(1), pp. 45–66. DOI: <https://doi.org/10.2174/1872210515666210120114504>
5. Asha, A.B.; Narain, R. Nanomaterials properties. Narain, R. Ed. *Polymer Science and Nanotechnology*. Elsevier, 2020, pp. 343–359. DOI: <https://doi.org/10.1016/B978-0-12-816806-6.00015-7>
6. Khanna, V.K. Nanomaterials and their properties. Khanna, V.K. Ed. *Integrated Nanoelectronics: Nanoscale CMOS, Post-CMOS and Allied Nanotechnologies*. Springer: New Delhi, 2016, pp. 25–41. DOI: [https://doi.org/10.1007/978-81-322-3625-2\\_3](https://doi.org/10.1007/978-81-322-3625-2_3)
7. Varghese, R.J.; Sakho, El H.M.; Parani, S.; Thomas, S.; Oluwafemi, O.S.; Wu, J. Introduction to nanomaterials: synthesis and applications. Thomas, S.; Kalarikkal, N.; Wu, J.; Sakho, El H.M.; Oluwafemi, O.S. Eds. *Nanomaterials for Solar Cell Applications*. Elsevier, 2019, pp. 75–95. DOI: <https://doi.org/10.1016/B978-0-12-813337-8.00003-5>
8. Sharma, J.N.; Pattadar, D.K.; Mainali, B.P.; Zamborini, F.P. Size determination of metal nanoparticles based on electrochemically measured surface-area-to-volume ratios. *Analytical Chemistry*, 2018, 90(15), pp. 9308–9314. DOI: <https://doi.org/10.1021/acs.analchem.8b01905>
9. Shaji, A.; Zachariah, A.K. Surface area analysis of nanomaterials. Thomas, S.; Thomas, R.; Zachariah, A.; Mishra, R. Eds. *Thermal and Rheological Measurement Techniques for Nanomaterials Characterization*. Elsevier, 2017, pp. 197–231. DOI: <https://doi.org/10.1016/B978-0-323-46139-9.00009-8>
10. El-Morsy, M.A.; Awwad, N.S.; Ibrahim, H.A.; Farea, M.O. Optical and electrical conductivity properties of ZnO and TiO<sub>2</sub> nanoparticles scattered in PEO-PVA for electrical devices. *Results in Physics*, 2023, 50, 106592, pp. 1–7. DOI: <https://doi.org/10.1016/j.rinp.2023.106592>
11. Mehra, R.M. Electronic and mechanical properties of nanoparticles. Saxena, A.; Bhattacharya, B.; Caballero-Briones, F. Eds. *Applications of Nanomaterials for Energy Storage Devices*. CRC Press, 2022, pp. 127–141. DOI: <https://doi.org/10.1201/9781003216308>
12. Rahman, M.T.; Hoque, M.A.; Rahman, G.T.; Gafur, M.A.; Khan, R.A.; Hossain, M.K. Study on the mechanical, electrical, and optical properties of metal-oxide nanoparticles dispersed unsaturated polyester resin nanocomposites. *Results in Physics*, 2019, 13, 102264, pp. 1–8. DOI: <https://doi.org/10.1016/j.rinp.2019.102264>
13. Mahmood, Z.H.; Jarosova, M.; Kzar, H.H.; Machek, P.; Zaidi, M.; Khalaji, A.D.; Khlewee, I.H.; Altimari, U.S.; Mustafa, Y.F.; Kadhim, M.M. Synthesis and characterization of Co<sub>3</sub>O<sub>4</sub> nanoparticles: application as performing anode in Li-ion batteries. *Journal of the Chinese Chemical Society*, 2022, 69(4), pp. 657–662. DOI: <https://doi.org/10.1002/jccs.202100525>
14. Maghrabie, H.M.; Elsaid, K.; Sayed, E.T.; Radwan, A.; Abo-Khalil, A.G.; Rezk, H.; Abdelkareem, M.A.; Olabi, A.G. Phase change materials based on nanoparticles for enhancing the performance of solar photovoltaic panels: A review. *Journal of Energy Storage*, 2022, 48, 103937, pp. 1–18. DOI: <https://doi.org/10.1016/j.est.2021.103937>
15. He, Z.; Zhang, Z.; Bi, S. Nanoparticles for organic electronics applications. *Materials Research Express*, 2020, 7(1), 012004, pp. 1–13. DOI: <https://doi.org/10.1088/2053-1591/ab636f>
16. Jan, H.; Shah, M.; Andleeb, A.; Faisal, S.; Khattak, A.; Rizwan, M.; Drouet, S.; Hano, Ch.; Abbasi, B.H. Plant-based synthesis of zinc oxide nanoparticles (ZnO-NPs) using aqueous leaf extract of *Aquilegia pubiflora*: Their antiproliferative activity against HepG2 cells inducing reactive oxygen species and other *in vitro* properties. *Oxidative Medicine and Cellular Longevity*, 2021, 1, 4786227, pp. 1–14. DOI: <https://doi.org/10.1155/2021/4786227>
17. Daniel, A.I.; Keyster, M.; Klein, A. Biogenic zinc oxide nanoparticles: A viable agricultural tool to control plant pathogenic fungi and its potential effects on soil and plants. *Science of the Total Environment*, 2023, 897, 165483, pp. 1–9. DOI: <https://doi.org/10.1016/j.scitotenv.2023.165483>
18. Yadav, A.; Jangid, N.K.; Khan, A.U. Biogenic synthesis of ZnO nanoparticles from *Evolvulus alsinoides* plant extract. *Journal of Umm Al-Qura University for Applied Sciences*, 2024, 10(1), pp. 51–57. DOI: <https://doi.org/10.1007/s43994-023-00076-z>
19. Demir, C.; Aygun, A.; Gunduz, M.K.; Altınok, B.Y.; Karahan, T.; Meydan, I.; Halvacı, E.; Tiri, R.N.E.; Sen, F. Production of plant-based ZnO NPs by green synthesis; anticancer activities and photodegradation of methylene red dye under sunlight. *Biomass Conversion and Biorefinery*, 2024, pp. 1–16. DOI: <https://doi.org/10.1007/s13399-024-06172-2>
20. Chandrasekaran, S.; Anbazhagan, V. Green synthesis of ZnO and V-Doped ZnO nanoparticles using *Vinca rosea* plant leaf for biomedical

- applications. Applied Biochemistry and Biotechnology, 2024, 196(1), pp. 50–67. DOI: <https://doi.org/10.1007/s12010-023-04546-2>
21. Nava, O.J.; Soto-Robles, C.A.; Gómez-Gutiérrez, C.M.; Vilchis-Nestor, A.R.; Castro-Beltrán, A.; Olivas, A.; Luque, P.A. Fruit peel extract mediated green synthesis of zinc oxide nanoparticles. Journal of Molecular Structure, 2017, 1147, pp. 1–6. DOI: <https://doi.org/10.1016/j.molstruc.2017.06.078>
  22. Ravbar, M.; Kunčič, A.; Matoh, L.; Možina, S.S.; Šala, M.; Šuligoj, A. Controlled growth of ZnO nanoparticles using ethanolic root extract of Japanese knotweed: photocatalytic and antimicrobial properties. RSC Advances, 2022, 12(48), pp. 31235–31245. DOI: <https://doi.org/10.1039/d2ra04202a>
  23. Tripathi, P.K.; Barthwal, A.S.; Sati, S.C. Plant mediated synthesis of zinc oxide nanoparticles and evaluation of its anti-microbial and anti-oxidant activities. UJPAH, 2021, 1(30), pp. 67–74. DOI: [https://doi.org/10.51129/UJPAH-JUNE2021-30-1\(10\)](https://doi.org/10.51129/UJPAH-JUNE2021-30-1(10))
  24. Parra, M.R.; Haque, F.Z. Aqueous chemical route synthesis and the effect of calcination temperature on the structural and optical properties of ZnO nanoparticles. Journal of Materials Research and Technology, 2014, 3(4), pp. 363–369. DOI: <https://doi.org/10.1016/j.jmrt.2014.07.001>
  25. Quevedo Robles, R.V.; Vilchis Nestor, A.R.; Luque Morales, P.A. Synthesis of zinc oxide semiconductor nanoparticles using natural extract: a systematic evaluation of cationic dye photodegradation influenced by extract concentration, catalyst dose, and pH. Environmental Science and Pollution Research, 2024, 31, pp. 63161–63175. DOI: <https://doi.org/10.1007/s11356-024-35431-y>
  26. Li, D.; Ti, P.; Huang, L.; Chen, X.; Zhu, Q.; Chen, J.; Yuan, Q. High thermal conductivity regenerated cellulose/carboxylated carbon nanotubes composite films with semi-insulating properties prepared via ionic coordination and hydrothermal synthesis of zinc oxide. International Journal of Biological Macromolecules, 2024, 264(1), 130004, pp. 1–11. DOI: <https://doi.org/10.1016/j.ijbiomac.2024.130004>
  27. Gouda, M.; Mohamed, H.A.; Abou Taleb, M.F.; Alqahtani, N.K. Antimicrobial zinc oxide/polymer nanocomposites for the removal of toxic textile dye. Cellulose, 2024, 31(14), pp. 8935–8959. DOI: <https://doi.org/10.1007/s10570-024-06124-z>
  28. Rini, A.S.; Syahrul, M.; Rati, Y. Photocatalytic performance of sulfur-doped zinc oxide: green synthesis via matoa leaf extract mediation. Advances in Natural Sciences: Nanoscience and Nanotechnology, 2024, 16(1), 015008, pp. 1–9. DOI: <https://doi.org/10.1088/2043-6262/ada007>
  29. Ammu, V.K.; Pushpadass, H.A.; Franklin, M.E.E.; Duraisamy, R. Biosynthesis of zinc oxide nanoparticles using *Carica papaya* and *Cymbopogon Citratus* leaf extracts: a comparative investigation of morphology and structures. Journal of Molecular Structure, 2025, 1323, 140737, pp. 1–10. DOI: <https://doi.org/10.1016/j.molstruc.2024.140737>
  30. Achamo, T.; Zereffa, E.A.; Murthy, H.A.; Ramachandran, V.P.; Balachandran, R. Phyto-mediated synthesis of copper oxide nanoparticles using *Artemisia abyssinica* leaf extract and its antioxidant, antimicrobial, and DNA binding activities. Green Chemistry Letters and Reviews, 2022, 15(3), pp. 598–614. DOI: <https://doi.org/10.1080/17518253.2022.2121620>
  31. Jalil, P.J.; Mhamedsharif, R.M.; Shnawa, B.H.; Hamad, S.M.; Aspoukeh, P.; Wsu, K.W.; Mhamedsharif, S.M.; Ahmed, M.H. Biosynthesis of ZnO nanoparticles using *Washingtonia filifera* seed extract and assessment of their anti-inflammatory and antimicrobial efficacy. Journal of Cluster Science, 2025, 36(1), 31, pp. 1–19. DOI: <https://doi.org/10.1007/s10876-024-02761-3>
  32. Shnawa, B.H.; Jalil, P.J.; Al-Ezzi, A.; Mhamedsharif, R.M.; Mohammed, D.A.; Biro, D.M.; Ahmed, M.H. Evaluation of antimicrobial and antioxidant activity of zinc oxide nanoparticles biosynthesized with *Ziziphus spina-christi* leaf extracts. Journal of Environmental Science and Health, Part C, 2024, 42(2), pp. 93–108. DOI: <https://doi.org/10.1080/26896583.2023.2293443>
  33. Hayat, K.; Din, I.U.; Alam, K.; Khan, F.U.; Khan, M.; Mohamed, H.I. Green synthesis of zinc oxide nanoparticles using plant extracts of *Fumaria officinalis* and *Peganum harmala* and their antioxidant and antibacterial activities. Biomass Conversion and Biorefinery, 2025, 15, pp. 9565–9579. DOI: <https://doi.org/10.1007/s13399-024-05804-x>
  34. Aydin Acar, A.; Gencer, M.A.; Pehlivanoglu, S.; Yesilot, S.; Donmez, S. Green and eco-friendly biosynthesis of zinc oxide nanoparticles using *Calendula officinalis* flower extract: wound healing potential and antioxidant activity. International Wound Journal, 2024, 21(1), e14413, pp. 1–11. DOI: <https://doi.org/10.1111/iwj.14413>
  35. Zewde, D.; Geremew, B. Biosynthesis of ZnO nanoparticles using *Hagenia abyssinica* leaf extracts; their photocatalytic and antibacterial activities. Environmental Pollutants and Bioavailability, 2022, 34(1), pp. 224–235. DOI: <https://doi.org/10.1080/26395940.2022.2081261>
  36. Ifeanyichukwu, U.L.; Fayemi, O.E.; Ateba, C.N. Green synthesis of zinc oxide nanoparticles from pomegranate (*Punica granatum*) extracts and characterization of their antibacterial activity. Molecules, 2020, 25(19), 4521, pp. 1–22. DOI: <https://doi.org/10.3390/molecules25194521>
  37. Janaki, A.C.; Sailatha, E.; Gunasekaran, S. Synthesis, characteristics and antimicrobial activity of ZnO nanoparticles. Spectrochimica Acta Part A: Molecular and Biomolecular Spectroscopy, 2015, 144, pp. 17–22. DOI: <https://doi.org/10.1016/j.saa.2015.02.041>
  38. Al Bustany, A.; Abbas, H.; Al-Omar, A.A.; Soubh, A.M.; Shriteh, T.; Al Mahfoud, H.

- Antibacterial efficacy of zinc oxide nanoparticles synthesized by green and chemical methods. *Environmental Health Engineering and Management Journal*, 2024, 11(4), pp. 409–418.  
DOI: <https://doi.org/10.34172/ehem.2024.40>
39. Karatepe, P.; Akgöl, M.; Bayrak, S.; İncili, G.K. In-vitro antimicrobial activity of ZnO nanoparticles produced by hydrothermal method against some foodborne pathogens. *Turkish Journal of Agriculture - Food Science and Technology*, 2024, 12(s2), pp. 2266–2271.  
DOI: <https://doi.org/10.24925/turjaf.v12is2.2266-2271.7002>
40. Azeem, M.; Siddique, M.H.; Imran, M.; Zubair, M.; Mumtaz, R.; Younas, M.; Abdel-Maksoud, M.A.; El-Tayeb, M.A.; Rizwan, M.; Yong, J.H. Assessing anticancer, antidiabetic, and antioxidant capacities in green-synthesized zinc oxide nanoparticles and solvent-based plant extracts. *Heliyon*, 2024, 10(14), e34073, pp. 1–12.  
DOI: <https://doi.org/10.1016/j.heliyon.2024.e34073>
41. Nagajyothi, P.C.; Cha, S.J.; Yang, I.J.; Sreekanth, T.V.M.; Kim, K.J.; Shin, H.M. Antioxidant and anti-inflammatory activities of zinc oxide nanoparticles synthesized using *Polygala tenuifolia* root extract. *Journal of Photochemistry and Photobiology B: Biology*, 2015, 146, pp. 10–17.  
DOI: <https://doi.org/10.1016/j.jphotobiol.2015.02.008>
42. Sivasankarapillai, V.S.; Krishnamoorthy, N.; Eldesoky, G.E.; Wabaidur, S.M.; Islam, M.A.; Dhanusuraman, R.; Ponnusamy, V.K. One-pot green synthesis of ZnO nanoparticles using *Scoparia Dulcis* plant extract for antimicrobial and antioxidant activities. *Applied Nanoscience*, 2023, 13, pp. 6093–6103.  
DOI: <https://doi.org/10.1007/s13204-022-02610-7>
43. Jamil, Y.M.; Al-Maydama, H.M.; Al-Hakimi, A.N.; Al-Mahwit, G.Y.; Ibrahim, H.M.; Al-Akhali, B. The characterization, antibacterial and antioxidant of phytosynthesized zinc oxide nanoparticles using *Aloe fleurentinorum* leaves extract. *Sana'a University Journal of Applied Sciences and Technology*, 2024, 2(4), pp. 339–347.  
DOI: <https://doi.org/10.59628/jast.v2i4.1011>
44. Kumar, H.; Bhardwaj, K.; Nepovimova, E.; Kuča, K.; Singh Dhanjal, D.; Bhardwaj, S.; Bhatia, S. K.; Verma, R.; Kumar, D. Antioxidant functionalized nanoparticles: A combat against oxidative stress. *Nanomaterials*, 2020, 10(7), 1334, pp. 1–26.  
DOI: <https://doi.org/10.3390/nano10071334>